4D simultaneous tissue and blood flow Doppler imaging: revisiting cardiac Doppler index with single heart beat 4D ultrafast echocardiography

Clement Papadacci, V Finel, O Villemain, G Goudot, J. Provost, E. Messas, M. Tanter, Mathieu Pernot

4D simultaneous tissue and blood flow Doppler imaging:

Revisiting cardiac Doppler index with single heart beat 4D ultrafast echocardiography

C. Papadacci[a] PhD, V. Finel[a], O. Villemain[abc] MD PhD, G. Goudot[a] MD, J. Provost[a] PhD, E. Messas[cd] MD PhD, M. Tanter[a] PhD and M. Pernot[a] PhD

[a]Physics For Medicine Paris, INSERM U1273, ESPCI Paris, PSL Research University, CNRS UMR 7587

[b]M3C-Necker Enfants malades, AP-HP, Paris, France

[c]Paris Descartes University, USPC Sorbonne Paris Cité, Paris, France

[d]INSERM U970 PARCC, Hôpital Européen Georges-Pompidou, AP-HP, Paris, France

Corresponding author

Clement Papadacci / Mathieu Pernot

Abstract (250 words)

Objectives

The goal of this study was to demonstrate the feasibility of semi-automatic evaluation of cardiac Doppler indices in a single heartbeat on human hearts by performing 4D ultrafast echocardiography with a dedicated sequence of 4D simultaneous tissue and blood flow Doppler imaging.

Background

4D echocardiography has the potential to improve the quantification of major cardiac indices by providing more reproducible and less user dependent measurements such as the quantification of left ventricle (LV) volume. The evaluation of Doppler indices, however, did not benefit yet from 4D echocardiography because of limited volume rates achieved in conventional volumetric color Doppler imaging but also because spectral Doppler estimation is still restricted to a single location.

Methods

High volume rate (5200 volume/s) transthoracic simultaneous tissue and blood flow Doppler acquisitions of three human LV were performed using a 4D ultrafast echocardiography scanner prototype during a single heartbeat. 4D color flow, 4D tissue Doppler cineloops and spectral Doppler at each voxel were computed. LV outflow tract, mitral inflow and basal inferoseptal locations were automatically detected. Doppler indices were derived at these locations and were compared against clinical 2D echocardiography.

Results

Blood flow Doppler indices E (early filling), A (atrial filling), E/A ratio, S (systolic ejection) and cardiac output were assessed on the three volunteers. Simultaneous tissue Doppler indices e' (mitral annular velocity peak), a' (late velocity peak), e'/a' ratio, s' (systolic annular velocity peak), E/e' ratio were also estimated. Standard deviations on three independent acquisitions were averaged over the indices and was found to be inferior to 4% and 8.5% for Doppler flow and tissue Doppler indices, respectively. Comparison against clinical 2D echocardiography gave a p value larger than 0.05 in average indicating no significant differences.

Conclusions

4D ultrafast echocardiography can quantify the major cardiac Doppler indices in a single heart beat acquisition.

Key Words (max 6)

4D echocardiography

4D ultrafast echocardiography

Doppler index

Cardiac function

Abbreviations list (max 10)

4DE: Four dimensional echocardiography

4DUE: Four dimensional ultrafast echocardiography

CO: Cardiac output

ECG: electrocardiogram

LV: left ventricle

LVOT: Left ventricular outflow tract

PW Doppler: Pulse wave Doppler

RV: right ventricle

SVD: singular value decomposition

TDI: Tissue Doppler imaging

Introduction

Four dimensional echocardiography (4DE), or animated three dimensional echocardiography, has become a powerful tool for the evaluation of the cardiac function (1). It can provide reliable measurements of cardiac function index such as left ventricular volumes (2) or ejection fraction (3) and is often considered less user dependent than 2D echocardiography (3). Moreover, post-acquisition measurements with 4DE has the potential to become fully automated and therefore to reduce even more the user dependency (4). Current evaluation of cardiac function with 4DE remains however currently limited to the anatomical measurements performed on the volumetric images. Volumetric Color flow Doppler echocardiography is also possible but is highly limited by the low volume rate offered by Doppler 4DE (5). Acquisitions are therefore limited to small volumes or require long acquisitions with ECG gating (5). More importantly, 4DE Doppler imaging is limited to color flow visualization and does not allow the quantification of major Doppler indices that require spectral Doppler estimation.

All the functional Doppler indices are yet recommended to be explored with 2D acquisitions, because of 4D frame rate limitations (6). For each index, challenging manual manipulation must be performed by a trained cardiologist or sonographer. Variability of Doppler measurements is therefore highly dependent on the expertise of the sonographer (7). In addition, the entire examination is time

consuming since each Doppler measurement can take a noticeable amount of time (and sometimes questionable results) due to manipulations and manual selection of regions of interest.

In biomedical research, ultrafast ultrasound has been developed for more than two decades (8) in order to perform ultrasound imaging at 6000 images/s. The method relies on the emission of unfocused wave to insonifiate all the medium in a few transmit. Recently, ultrafast imaging was extended to 4D ultrasound imaging using matrix transducer arrays to achieve up to 6000 volumes/s of the human body. Doppler flow imaging (9), elastography (10–12) and vascular imaging (13) were the first applications to benefit from 4D ultrafast imaging. In the heart, 4D ultrasound ultrafast imaging was leveraged to image, fiber orientation mapping (14), blood flow in the entire left ventricle of a human volunteer (9) and tissue displacement in canine's hearts (15). One interesting property of ultrafast imaging is that it enables quantifications in the entire field of view. In the case of Doppler blood flow, one spectrogram can be retrieved from each voxel as if Pulse Wave (PW) Doppler was performed simultaneously at each location of the volume (16). Similarly, for tissue Doppler imaging (TDI), one tissue velocity curve can be derived from each pixel simultaneously with high temporal resolution (17).

In this study, we first developed a new 4D simultaneous tissue and blood flow Doppler acquisition to retrieve 4D color Doppler and 4D TDI in entire volumes during a single heartbeat using a spatio-temporal clutter filtering based on singular value decomposition. From these volumes, Doppler spectra and a tissue velocity curve were automatically extracted at the Left Ventricular Outflow Tract (LVOT), across the mitral valve and at the basal septum locations, respectively. Blood flow Doppler indices E (early filling), A (atrial filling), E/A ratio and S (systolic ejection) were assessed on the three volunteers. Simultaneous tissue Doppler indices e' (mitral annular velocity peak), a' (late velocity peak), e'/a' ratio, s' (systolic annular velocity peak), E/e' ratio were also estimated. Cardiac output (CO) was quantified without making any geometrical assumptions. These major left ventricular Doppler indices were quantified in three human volunteers. Each volunteer was scanned three times to assess reproducibility. The measurements were compared to indices measured on a 2D clinical ultrasound system.

Methods

General flow chart of four dimensional ultrafast echocardiography (4DUE) method is displayed in figure 1. Ultrafast acquisition is first performed at a volume rate of 5200 v/s during 1.2 seconds (figure 1 (a)). Radio-frequency data stored in memory are used to beamform 6000 in-phase and quadrature components (IQ) data (figure 1 (b)).For visualization, 3D scan-conversion is applied to the data. A spatio-temporal clutter filtering is applied to IQ data to separate tissue signal from blood signal (figure 1 (c)). Spectral Doppler and tissue velocity curves are computed at each voxel of the cavity and myocardium, respectively. 4D TDI and 4D color Doppler are assessed. Automatic detection of locations of interest are processed based on maxima and minima maps from the 4D color Doppler (figure 1 (d)). Spectral Doppler images and tissue velocity curve at the LVOT, mitral inflow and basal inferospetum locations are used for quantifications (figure 1 (e)). Doppler indices are extracted from the images and curve (figure 1 (f)).

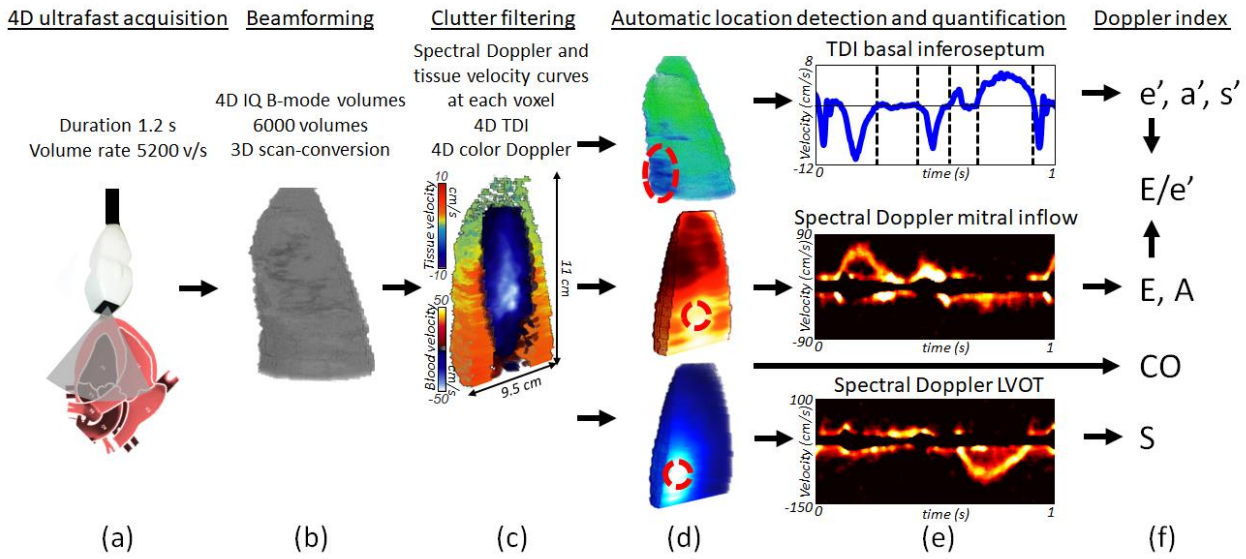

Figure 1: Flow chart of 4D ultrafast echocardiography (4DUE) method to retrieve cardiac indices. (a) Acquisition of thousands of volumes at ultrafast frame rate. (b) 4D in-phase and quadrature (IQ) B-mode beamforming. (c) Spatio-temporal clutter filtering was performed to assess spectral Doppler and tissue velocity curves for each voxel. 4D tissue Doppler imaging (TDI) and 4D color Doppler were computed. (d) Automatic detection of transvalvular flows. (e) Semi-automatic quantification on the TDI and the spectral Doppler. (f) Doppler Index assessment.

4D ultrafast acquisition

The left ventricle of three healthy human volunteers was imaged. A trained cardiologist positioned the matrix array probe with a real-time two dimensional B-mode image on the apical four-chamber view centered on the left ventricle. Ultrafast diverging wave acquisitions were performed during 1.2 seconds and electrocardiogram (ECG) was co-recorded during the acquisition.

A 2.25MHz matrix array probe (1024 elements, 0.3 mm pitch, Vermon, France) connected to an ultrasound device with 1024 channels in emission and receive was used. 6000 diverging waves were emitted at a rate of 5200 volumes per second. The pulse length was set to four cycles and a band pass receive filter with a center frequency around 2.25MHz was set in receive.

The acquisition was repeated three times for each volunteer to assess reproducibility and the third acquisition was performed by a second trained cardiologist. The three acquisitions for each volunteer were performed during the same day. The three volunteers were male with age of 24, 30 and 40 years old.

Mechanical index (MI), spatial peak temporal average intensity (ISPTA), spatial peak pulse average intensity (ISPPA) were measured in an acoustic measurement tank (Acertara, USA). MI = 0.8 - ISPTA = 365 mW/cm^2 – ISPPA = 51 W/cm^2 were measured. Therefore, the configuration was kept within the FDA safety recommendations for cardiac applications.

Beamforming

The virtual source position of the diverging waves was chosen to reach a 70° sector field of view according to (9,17). Radio-Frequency data sampled at a 9 MHz frequency was stored in memory for each diverging wave. Data were beamformed using a conventional delay and sum parallel algorithm implemented on Graphical Processing Unit (Nvidia Titan X), and converted into 4D IQ volumes of

70x70x470 pixels corresponding to 70°x70°x120mm volumes inducing a lateral resolution of 1° and an axial resolution of half-wavelength (342 μm) per voxel.

For volume visualization, 3D scan-conversion was applied to the data. 3D mask of the left ventricle cavity and myocardium were segmented manually by a trained cardiologist on 2D transverse slices from scan-converted B-mode volumes. Interpolation over depth was performed to get the 3D masks. The volume rendering was performed using Amira software (Visualization, Sciences Group, Burlington, MA).

Clutter filtering

4D tissue and color Doppler were computed by performing a spatio-temporal clutter filtering based on a singular value decomposition (SVD) to separate signal from the tissue and the signal from the blood flow as it is done by Demene et al in (18). The first 800 eigenvectors were associated to tissue whereas the last 5200 eigenvectors were associated to blood flow. In this study, the sliding window approach was not used.

4D tissue Doppler imaging was computed by performing 1D cross-correlation on demodulated SVD-filtered IQ volumes to obtain volumes of tissue volume-to-volume axial displacements. A butter-worth low-pass filtering with a 100Hz cut-off frequency was applied. At each voxel, a tissue displacement curve was assessed.

Short-time Fourier transform was performed in time at every voxels of the blood flow SVD-filtered IQ volumes using a 60 sample-sliding window to retrieve spectral Doppler for each voxel.

4D color Doppler was obtained by calculating the mean Doppler velocity (Spectrum 1^{st} moment) on demodulated SVD-filtered IQ volumes after applying a directional filter and a dealiasing filter for the highest speeds (19). Directional filter and dealiasing algorithm are important to estimate the mean Doppler velocity. The idea of the directional filter and dealiasing filter is simple. At a given time inside a voxel, it is unlikely to have both upward and downward blood flow in the same time. Because the blood flow direction is unique, it enables to have an efficient bandwidth from –fs to fs with a sampling frequency of only fs (where fs = 1/volume rate). In practice, the aliased part in the spectrum is moved to the opposite side.

Automatic location detection and quantification

Blood velocity minima and maxima over time were detected to get 3D blood flow maps of the ejection and the rapid filling, respectively. Blood velocity minimum and maximum over time and space were detected to automatically derive in three dimensions the spatial coordinates of the highest ejection and rapid filling blood flow speed locations. From these locations, two spectral Doppler images were generated corresponding to the LVOT and mitral inflow locations.

Tissue velocity minima over time was mapped in 3D to visualize early relaxation. Basal inferoseptal location was automatically detected by using the myocardial tissue next to the spatial coordinates of the highest ejection location corresponding to the aortic valve. From this location, a tissue velocity curve was generated.

Doppler index estimation

Manual selection on the spectrograms and tissue velocity was performed by a trained cardiologist to assess indices. From LVOT spectral Doppler, the S index corresponding to systolic ejection was measured. From mitral inflow spectral Doppler, E index corresponding to early filling, A index corresponding to atrial filling and E/A ratio were also measured.

From the tissue velocity curve assessed at the basal inferoseptum location, indices s' corresponding to systolic annular velocity peak, e' corresponding to mitral annular velocity peak, a' corresponding to late velocity peak, e'/a' ratio and E/e' ratio were measured using manual selection.

Finally Cardiac Output (CO) was measured using 4D color Doppler data. CO is classically defined as the product of Stroke Volume (SV) with Heart Rhythm (HR) (20):

$$CO = SV \times HR$$

In our case, the SV was obtained without any geometrical assumption by integrating the mean Doppler velocity $v_{dop}(s,t)$ temporally over the systolic phase t_{sys} and spatially over the entire Cross Section Area (CSA), at a depth corresponding to the aortic valve location. There was no need of angular correction of the Doppler measurement because the integration surface was always perpendicular to the beam axis as it is done in (21).

such as:

$$SV = \int_{t=0}^{t=t_{sys}} \int_{S=0}^{S=CSA} v_{dop}(s,t)\, \vec{n}.\overrightarrow{ds}\, dt$$

Where $\vec{n}$ is the normalized vector in the direction of the ultrasound beam and $\overrightarrow{ds}$ is the infinitesimal surface oriented towards the probe.

Comparison against clinical acquisition using 2D conventional echocardiography

The three normal subjects were scanned by a trained cardiologist using a clinical ultrasound system (Acuson SC2000 system; Siemens Medical Solutions, USA). Two PW Doppler acquisitions and a TDI acquisition were performed successively at the mitral annulus, the LVOT and the basal inferoseptal location, respectively. Doppler flow profiles were recorded and the different phases of the heart were visualized. From these spectrums E, A, E/A, S, e', a', e'/a', s' and E/e' index were measured. ECG was co-recorded during the acquisition. Comparison of Doppler parameters were made with the Student 2-tailed paired t-test (table 1). The level of significance was set at an alpha level of ≤0.05. Analyses were conducted using MedCalc software (MedCalc Software, Mariakerke, Belgium).

Results

4D color Doppler and 4D tissue velocity

4D color Doppler and tissue velocity were assessed within the same acquisition. The different cardiac phases were visualized for the three volunteers. Figure 2 and the cine loop attached display the results for one volunteer. Positive blood flow and tissue velocities are represented in red (going towards the probe). Negative blood flow and tissue velocities are represented in blue (going away from the probe). During rapid inflow, blood flows upward (red) and tissue relaxation induces a downward motion (blue). Diastasis phase is characterized by vortex patterns in the blood and limited motion in the myocardium. During atrial systole, the atrium ejects the remaining blood in the ventricle (red) and induces a rapid motion in the myocardium also known as 'atrial kick' (blue). Pre-ejection displays transitory waves in the myocardium and turbulence in the blood. Finally, during the ejection the blood flows downwards (blue) while the myocardium contraction induces basal tissue to move upward (orange) and apical tissue to slightly move downward (light blue). These phases are displayed in figure 2 (a). At each voxel of the volume, Doppler spectrograms and tissue velocity plots can be derived. Two examples are displayed in figure 2 (b-c). The spectral Doppler and tissue velocity curve were taken arbitrarily in the cavity and myocardium respectively for illustration purposes.

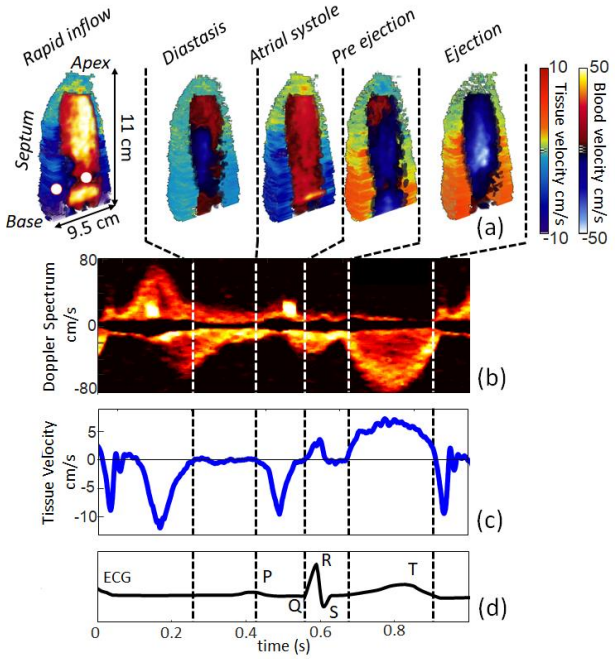

Figure 2: Simultaneous 4D color Doppler and 4D TDI of a human volunteer left ventricle in a single heartbeat. (a) Three dimensional representation of Color Doppler and tissue velocity in volumes allowing visualization of the cardiac phases. (b) Doppler spectrogram from one random voxel of the cardiac cavity and (c) tissue velocity curve from one voxel of the myocardium allow quantifications. (d) ECG is co-registered.

Automatic detection of LVOT and mitral inflow locations for blood flow index calculation

4D blood flow speed minima mapping corresponding to the ejection is displayed for one volunteer in figure 3 (a). Horizontal and transverse slices are presented and enabled the localization of the transaortic valvular flow. By automatically detecting the minimum over time and space, the location of the highest ejection speed was assessed. The Doppler spectrum corresponding to this location is displayed in figure 3 (b). From this spectrum, S index value was measured.

Similarly, 4D blood flow speed maxima mapping corresponding to the rapid filling is displayed in figure 3 (c). Mitral flow could also be visualized and localized. Maximum over time was detected and a spectrogram was displayed at this location (figure 3 (d)). From the spectrogram the E, A and E/A index were measured. S, E, A, E/A were measured on the three acquisitions of each volunteer. The results are summarized in Table 1.

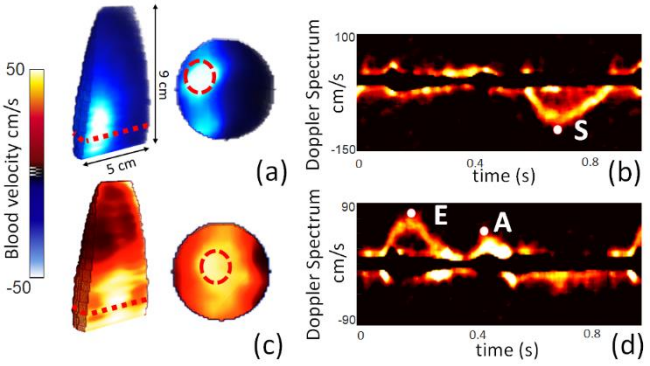

Figure 3: Automatic detection of absolute blood flow speed maxima during ejection (a) and early filling (c). (b-d) Associated spectrograms enable indices assessment.

Automatic detection of basal inferoseptum location for tissue index calculation

4D tissue Doppler minima mapping over time is displayed in figure 4. Previously calculated spatial coordinate of the LVOT was used to automatically derive the basal inferoseptal location (red dashed circle) as the closest tissue. Tissue velocity curve was averaged over a large area (figure 4 (b)) and s', e', a' and e'/a' were assessed for the three acquisitions of each volunteer (Table 1).

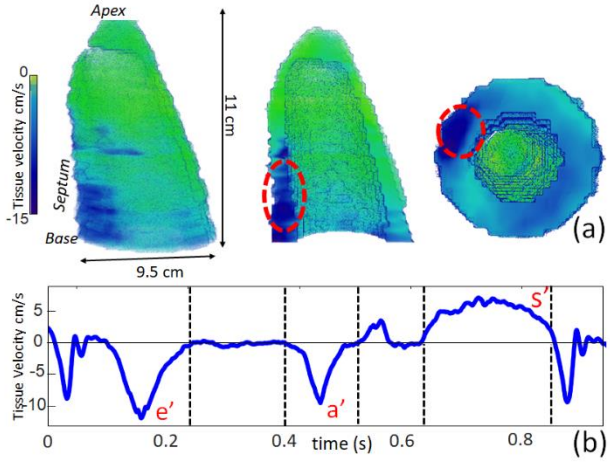

Figure 4: 4D tissue Doppler velocity minimum representation with tissue velocity curve associated to the basal inferoseptal location.

Cardiac Output calculation

From the 4D color Doppler, flow rate was derived without making any assumptions on the valve geometry as illustrated in figure 5. Blood flow speed was integrated over depth on 2D cross sections. Instantaneous flow rate over depth was assessed (figure 5 (b)). At a depth corresponding to the aortic valve location (green area in figure 5 (a)), CO was estimated by integrating the instantaneous flow rate over the systolic phase (figure 5 (c)). Results are summarized in Table 1.

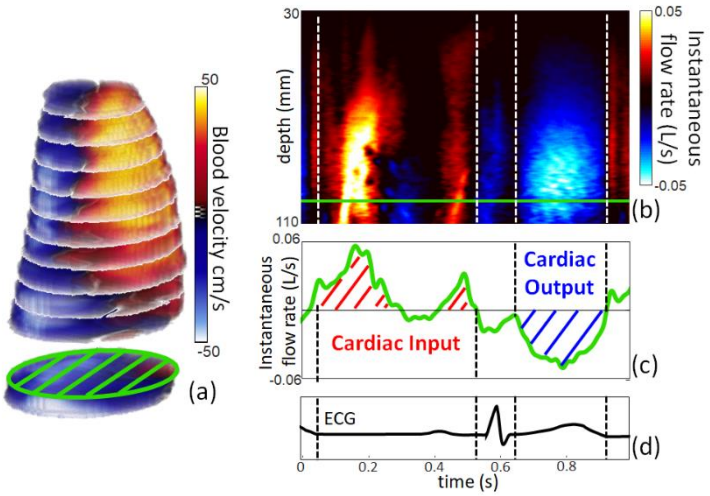

Figure 5: Cardiac output estimation. (a) Blood velocity is integrated over cross-sections along depth. Green cross section is situated at the LVOT. (b) Instantaneous flow rate is displayed over depth and (c)

at LVOT location. Cardiac output is estimated by integrating the instantaneous flow rate over systolic phase (d) according to ECG.

Mixed blood flow and tissue index

From E and e' assessments, E/e' was calculated in the same acquisition during the same heart beat for the three volunteers (Table 1).

Comparison between the acquisitions (4DUE and 2D echo)

The results of the three acquisitions for the three volunteers are presented in Table 1. For each volunteer, the indices calculated from the three independent 4DUE acquisitions were averaged and standard deviations were assessed. Small standard deviations, ~4% averaged over blood flow indices and ~8.5% over tissue indices, suggest good reproducibility between the acquisitions. Results from 2D echocardiography were also displayed in Table 1. P values were calculated to assess differences between 4DUE and 2D echo acquisitions. With a p value larger than 0.05 in average, no significant differences were observed between the two methods.

	volunteer # 1		*volunteer # 2*		*volunteer # 3*		*p*
Index	**4DUE**	**2D echo**	**4DUE**	**2D echo**	**4DUE**	**2D echo**	
E (cm/s)	77.8 ± 5.2	73	74.3 ± 1.0	72	83.6 ± 2.5	83	0.72
A (cm/s)	47.7 ± 0.9	48	51.4 ± 2.4	52	47.6 ± 1.4	49	0.65
E/A	1.6 ± 0.1	1.5	1.4 ± 0.1	1.4	1.8 ± 0.1	1.7	0.81
S (cm/s)	96.2 ± 4.3	98	121.3 ± 2.3	118	100.1 ± 2.5	100	0.53
e' (cm/s)	12.3 ± 0.1	12	9.4 ± 1.2	8	12.0 ± 0.4	12	0.49
a' (cm/s)	5.4 ± 0.6	5	9.4 ± 1.3	9	10.2 ± 0.1	10	0.61
e'/a'	2.3 ± 0.8	2.4	1.0 ± 0.1	0.9	1.2 ± 0.1	1.2	0.41
s' (cm/s)	7.1 ± 1.0	7	7.4 ± 1.1	9	5.7 ± 0.4	5.5	0.59
E/e'	6.3 ± 0.4	6	7.9 ± 1.0	9	7.0 ± 0.4	6.9	0.38
CO (L/min)	4.2 ± 0.1	4.6	4.1 ± 0.3	5.3	4.9 ± 0.3	5.5	0.42

Table 1: Comparison between indices assessed with the 4DUE acquisition and the clinical ultrasound system (2D echo) for the three volunteers. 4DUE index results were calculated as the average and standard deviation over the three acquisitions. P-values were calculated to analyze the results.

Cardiac evaluation with a clinical ultrasound system

Figure 6 displays the index assessment performed on one volunteer with the clinical ultrasound device. Clinical indices were derived and summarized in Table 1.

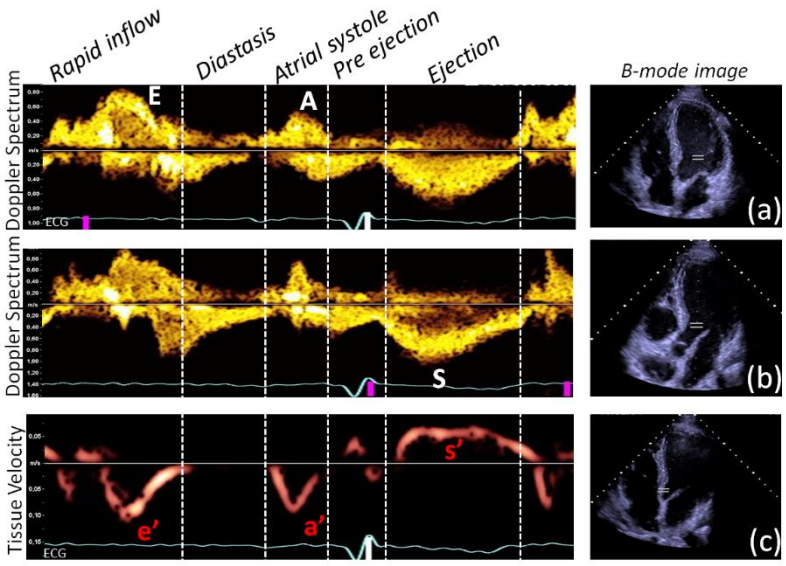

Figure 6: (a) Doppler spectrum at the mitral inflow and (b) at the LVOT. (c) Tissue velocity curve at the basal septum obtained with a clinical ultrasound system for one volunteer. The different phases of the cardiac cycle are identified and some clinical indices are measured.

Discussion

In this study, we demonstrate that 4DUE can be used for semi-automatic quantification of Doppler indices at every voxel of the entire field of view. Such a semi-automatic processing requires volumetric imaging to acquire the entire LV but also ultrafast imaging to perform quantification over a large field of view. The new method promises to simplify and accelerate clinical practice as well as removing most of the operator dependency.

More specifically, we developed 4DUE optimized for simultaneous 4D color Doppler and 4D tissue Doppler by acquiring thousands of volumes at a volume rate of 5200 volumes per second. A powerful spatio-temporal filter was used to remove the clutter signal and obtain high quality volumetric blood flow data. In contrast to temporal filters that separate tissue and blood signals only from their difference in velocities, the SVD is based on both spatial and temporal information and has been shown to achieve much better filtering (18). Automatization of the number of eigenvectors to separate the tissue from the blood signal could be performed as it is done in (22). By taking advantages of ultrafast imaging and volumetric acquisition, a novel processing was developed to automatically detect the regions of interest that clinicians usually select manually to assess cardiac indices. For instance, LVOT and mitral inflow locations were automatically detected by assessing the highest negative and positive flow speeds, respectively, from the 4D color Doppler. Spectrograms from these locations enabled to assess S, E, A and E/A indices in each acquisition of the three human volunteers. Similarly, basal septum location was automatically detected. A tissue velocity curve from this location was used to assess s', e', a' and e'/a' in each acquisitions of the three human volunteers. A unique feature of the method is also the capability of measuring both blood flow and tissue related indices (E/e') in a single heart beat which could be of a great interest for patients with atrial fibrillation (23).

The 4D nature of the acquisition also enabled the calculation of the CO without the need of making any assumption on the valve geometry, usually responsible of 3% to 12% error on the CO value (20), taking advantage that blood velocity can be assessed in entire cross-sections. CO at the aortic valve location was derived. Segmentation could also be used to spatially isolate the atrium and quantify regurgitations for instance.

The rich 4D information obtained with the method could provide other indices not calculated in this study such as Mitral Valve (MV) A duration or MV Deceleration Time.

The new method was tested by two trained cardiologists on three LV of human volunteers and the derived indices were successfully compared to the ones obtained with a clinical ultrasound system ($p>0.5$). The proposed method is of a great interest to clinical practice as it removes most of the manipulations like switching imaging modes thus reducing significantly the acquisition time and the operator dependency (~4% and ~8.5% variability averaged over Doppler flow and tissue indices respectively, on the three acquisitions performed on each volunteer). The only remaining manipulation would be the positioning of the probe in the apical four-chamber view at the beginning of the acquisition which would still require a specific training for the operator.

There are several limitations due to the transmit scheme. Firstly, due to the diverging nature of the transmitted wave, the penetration could be an issue for over-weighted patients as the wave may be attenuated faster. In these cases, other transmit strategies such as increasing the length of the transmitted pulse or using cascaded dual-polarity waves could be used (24). The receive aspect might be ameliorated as well with technological progress as more sensitive matrix array probe will be developed in the near future. Secondly, the overall image quality is degraded compared to a focused beam approach as only one diverging wave is used in this study. Sidelobes and clutter level may be also an issue for morphological representation. However, 4D B-mode volumes quality could be increased by using a dedicated sequence with spatial coherent compounding (9) or multi-line strategies (25) which would enable morphological and strain measurements to be performed (26). Thirdly, the matrix array probe used in this study is suboptimal for cardiac imaging. The number of elements are small (32x32 elements) compared to a clinical phased array probe (64-96 elements) resulting in a smaller aperture (9.6x9.6mm versus~19.2mm) and a lower image quality. Increasing the number of independent elements is challenging as it also implies increasing the number of channels of the ultrasound device. Extensive research is going on to reduce the number of channel in ultrafast imaging, by using dedicated micro-beamformer or by using sparse acquisition by turning off some elements. These strategies would allow to use larger matrix array probe and thus increase signal to noise ratio which is critical for Doppler imaging.

For many patients, valve leakage or stenosis could be present. In this cases, the volume rate of few thousands of volume per second might not be sufficient to resolve the very high blood flow speed. Dealiasing strategies with multiple pulse repetition frequencies, for example, could be used to retrieve the highest blood flow speeds as it is done in (27). Moreover, for patients with dilated heart, it may require to increase the beam sector by increasing the angular aperture.

This study focused on LV but could also be used on right ventricle (RV) by centering the probe on the RV using the 2D real-time B-mode images. The full heart could also be acquired in the same time by increasing the size of the imaging sector. We know that the impact of one ventricle on the adjacent ventricle plays a key role in cardiac function (28). To date, there is little published data describing imaging of ventricular-ventricular interactions. 4DUE could be a new and interesting tool to explore and understand this interaction.

To conclude, non-invasive evaluation of cardiac function remains central in clinical practice of cardiology, both in the evaluation of systolic and diastolic function. Although cardiac catheterization is the reference technique, cardiac ultrasound remains the routine non-invasive examination for detection and follow-up of cardiac diseases. The measurement of the ejection fraction and the evaluation of the left ventricle filling pressures, play indeed a diagnostic and prognostic role of major importance. However, due to the variability of ultrasound results, the use of alternative imaging

modality, such as MRI or nuclear cardiology, is sometimes required, although more difficult to achieve. Ultrasound limitations are induced by the two-dimensional imaging approach and the Doppler signal angular dependence which are responsible for inter-operator variability. For these reasons, 4DUE represents the next generation of cardiac imaging, overcoming theses current limitations, as it could become an accessible, fast, and robust imaging tool in daily practice. In this work, we particularly emphasized the measurement method based on a single cardiac cycle, reducing the variability of measurements, especially in cases of ectopic beats, a frequent situation that reduces the performance of 2D cardiac ultrasound.

Conclusions

In this study, 4DUE was developed to revisit the evaluation of the LV indices measured by ultrasound. The dedicated simultaneous tissue and blood flow Doppler sequence includes a new acquisition and processing flow chart. A few thousands of diverging waves were emitted at ultrafast volume rate on the LV of three normal subjects in order to achieve both 4D color Doppler and 4D tissue Doppler in volumes in a single heartbeat. From these volumes, methods were developed to semi-automatically detect region of interests associated to the indices E, A, E/A, S, e', a', e'/a', s', E/e' and cardiac output. 4DUE enables quantifications, thus spectrograms and tissue velocity curves were derived at each of the region of interest to enable index evaluation. 4DUE has the potential to improve patient care by accelerating examination time as well as result reproducibilities by removing most of the operator dependency.

Acknowledgments

This study was supported by the European Research Council under the European Union's Seventh Framework Programme (FP/2007-2013) / ERC Grant Agreement n° 311025 and the ANR-10-IDEX-0001-02 PSL* Research University. We acknowledge the ART (Technological Research Accelerator) biomedical ultrasound program of INSERM. The Titan X Pascal used for this research was donated by the NVIDIA Corporation.

References

1. Jenkins C., Bricknell K., Hanekom L., Marwick TH. Reproducibility and accuracy of echocardiographic measurements of left ventricular parameters using real-time three-dimensional echocardiography. J Am Coll Cardiol 2004;44(4):878–86. Doi: 10.1016/j.jacc.2004.05.050.
2. Thavendiranathan P., Liu S., Verhaert D., et al. Feasibility, Accuracy, and Reproducibility of Real-Time Full-Volume 3D Transthoracic Echocardiography to Measure LV Volumes and Systolic Function: A Fully Automated Endocardial Contouring Algorithm in Sinus Rhythm and Atrial Fibrillation. JACC Cardiovasc Imaging 2012;5(3):239–51. Doi: 10.1016/j.jcmg.2011.12.012.
3. Dorosz JL., Lezotte DC., Weitzenkamp DA., Allen LA., Salcedo EE. Performance of 3-Dimensional Echocardiography in Measuring Left Ventricular Volumes and Ejection Fraction: A Systematic Review and Meta-Analysis. J Am Coll Cardiol 2012;59(20):1799–808. Doi: 10.1016/j.jacc.2012.01.037.
4. Leung KYE., Bosch JG. Automated border detection in three-dimensional echocardiography: principles and promises. Eur J Echocardiogr J Work Group Echocardiogr Eur Soc Cardiol 2010;11(2):97–108. Doi: 10.1093/ejechocard/jeq005.
5. Perrin DP., Vasilyev NV., Marx GR., del Nido PJ. Temporal Enhancement of Three Dimensional Echocardiography by Frame Reordering. Jacc Cardiovasc Imaging 2012;5(3):300–4. Doi: 10.1016/j.jcmg.2011.10.006.
6. Nagueh SF., Smiseth OA., Appleton CP., et al. Recommendations for the Evaluation of Left Ventricular Diastolic Function by Echocardiography: An Update from the American Society of

Echocardiography and the European Association of Cardiovascular Imaging. J Am Soc Echocardiogr 2016;29(4):277–314. Doi: 10.1016/j.echo.2016.01.011.
7. Sahn DJ., DeMaria A., Kisslo J., Weyman AF. Recommendations regarding quantitation in M-mode echocardiography: results of a survey of echocardiographic measurements. Circulation 1978;58(6):1072–1083.
8. Tanter M., Fink M. Ultrafast imaging in biomedical ultrasound. IEEE Trans Ultrason Ferroelectr Freq Control 2014;61(1):102–19. Doi: 10.1109/TUFFC.2014.6689779.
9. Provost J., Papadacci C., Arango JE., et al. 3D ultrafast ultrasound imaging in vivo. Phys Med Biol 2014;59(19):L1. Doi: 10.1088/0031-9155/59/19/L1.
10. Papadacci C., Bunting EA., Konofagou EE. 3D Quasi-Static Ultrasound Elastography With Plane Wave In Vivo. IEEE Trans Med Imaging 2017;36(2):357–65. Doi: 10.1109/TMI.2016.2596706.
11. Gennisson J-L., Provost J., Deffieux T., et al. 4-D ultrafast shear-wave imaging. IEEE Trans Ultrason Ferroelectr Freq Control 2015;62(6):1059–65. Doi: 10.1109/TUFFC.2014.006936.
12. Correia et al. 3-D Elastic Tensor Imaging of isotropic and transverse isotropic soft tissues. PMB Press n.d.
13. Correia M., Provost J., Tanter M., Pernot M. 4D ultrafast ultrasound flow imaging: in vivo quantification of arterial volumetric flow rate in a single heartbeat. Phys Med Biol 2016;61(23):L48–61. Doi: 10.1088/0031-9155/61/23/L48.
14. Papadacci C., Finel V., Provost J., et al. Imaging the dynamics of cardiac fiber orientation in vivo using 3D Ultrasound Backscatter Tensor Imaging. Sci Rep 2017;7. Doi: 10.1038/s41598-017-00946-7.
15. Papadacci C., Bunting EA., Wan EY., Nauleau P., Konofagou EE. 3D Myocardial Elastography In Vivo. IEEE Trans Med Imaging 2017;36(2):618–27. Doi: 10.1109/TMI.2016.2623636.
16. Osmanski BF., Maresca D., Messas E., Tanter M., Pernot M. Transthoracic ultrafast Doppler imaging of human left ventricular hemodynamic function. IEEE Trans Ultrason Ferroelectr Freq Control 2014;61(8):1268–75. Doi: 10.1109/TUFFC.2014.3033.
17. Papadacci C., Pernot M., Couade M., Fink M., Tanter M. High-contrast ultrafast imaging of the heart. IEEE Trans Ultrason Ferroelectr Freq Control 2014;61(2):288–301. Doi: 10.1109/TUFFC.2014.6722614.
18. Demené C., Deffieux T., Pernot M., et al. Spatiotemporal Clutter Filtering of Ultrafast Ultrasound Data Highly Increases Doppler and fUltrasound Sensitivity. IEEE Trans Med Imaging 2015;34(11):2271–85. Doi: 10.1109/TMI.2015.2428634.
19. Demené C., Pernot M., Biran V., et al. Ultrafast Doppler reveals the mapping of cerebral vascular resistivity in neonates. J Cereb Blood Flow Metab Off J Int Soc Cereb Blood Flow Metab 2014;34(6):1009–17. Doi: 10.1038/jcbfm.2014.49.
20. Huntsman LL., Stewart DK., Barnes SR., Franklin SB., Colocousis JS., Hessel EA. Noninvasive Doppler determination of cardiac output in man. Clinical validation. Circulation 1983;67(3):593–602.
21. Papadacci C., Zordan C., Tanter M., Pernot M. Quantitative Cardiac Output Assessment Using 4D Ultrafast Doppler Imaging: An in Vitro Study. 2018 IEEE Int Ultrason Symp IUS 2018:1–4.
22. Baranger J., Arnal B., Perren F., Baud O., Tanter M., Demene C. Adaptive Spatiotemporal SVD Clutter Filtering for Ultrafast Doppler Imaging Using Similarity of Spatial Singular Vectors. IEEE Trans Med Imaging 2018;37(7):1574–86. Doi: 10.1109/TMI.2018.2789499.
23. Kusunose K., Yamada H., Nishio S., et al. Clinical Utility of Single-Beat E/e' Obtained by Simultaneous Recording of Flow and Tissue Doppler Velocities in Atrial Fibrillation With Preserved Systolic Function. JACC Cardiovasc Imaging 2009;2(10):1147–56. Doi: 10.1016/j.jcmg.2009.05.013.
24. Zhang Y., Guo Y., Lee W. Ultrafast Ultrasound Imaging With Cascaded Dual-Polarity Waves. IEEE Trans Med Imaging 2018;37(4):906–17. Doi: 10.1109/TMI.2017.2781261.
25. Cikes M., Tong L., Sutherland GR., D'hooge J. Ultrafast cardiac ultrasound imaging: technical principles, applications, and clinical benefits. JACC Cardiovasc Imaging 2014;7(8):812–23. Doi: 10.1016/j.jcmg.2014.06.004.

26. Mor-Avi V., Jenkins C., Kühl HP., et al. Real-Time 3-Dimensional Echocardiographic Quantification of Left Ventricular Volumes: Multicenter Study for Validation With Magnetic Resonance Imaging and Investigation of Sources of Error. JACC Cardiovasc Imaging 2008;1(4):413–23. Doi: 10.1016/j.jcmg.2008.02.009.
27. Posada D., Poree J., Pellissier A., et al. Staggered Multiple-PRF Ultrafast Color Doppler. IEEE Trans Med Imaging 2016;35(6):1510–21. Doi: 10.1109/TMI.2016.2518638.
28. Friedberg MK. Imaging Right-Left Ventricular Interactions. JACC Cardiovasc Imaging 2018;11(5):755–71. Doi: 10.1016/j.jcmg.2018.01.028.